A hybrid smoothed finite element method (H-SFEM) to solid mechanics problems

Xu Xu [1, 2], Yuantong Gu [2], Guirong Liu[3]

[1] College of Mathematics, Jilin University, 2699 Qianjin Street, Changchun 130012, P. R. China.
[2] School of Engineering Systems, Queensland University of Technology, Brisbane, QLD4001, Australia

[3]School of Aerospace systems, University of Cincinnati, Cincinnati, OH-45221-0070, USA

Abstract: In this paper, a hybrid smoothed finite element method (H-SFEM) is developed for solid mechanics problems by combining techniques of finite element method (FEM) and Node-based smoothed finite element method (NS-FEM) using a triangular mesh. A parameter α is equipped into H-SFEM, and the strain field is further assumed to be the weighted average between compatible stains from FEM and smoothed strains from NS-FEM. We prove theoretically that the strain energy obtained from the H-SFEM solution lies in between those from the compatible FEM solution and the NS-FEM solution, which guarantees the convergence of H-SFEM. Intensive numerical studies are conducted to verify these theoretical results and show that (1) the upper and lower bound solutions can always be obtained by adjusting α; (2) there exists a preferable α at which the H-SFEM can produce the ultrasonic accurate solution.

Keywords: Meshfree methods, point interpolation method, superconvergence, upper bound solution.

1 Introduction

The finite element method (FEM) is well developed, and is currently the dominant numerical approach for solids and structures. Most of FEM models are displacement methods based on the potential energy principle, in which the displacement is the primary variable. Displacement-based fully compatible FEM usually has the "overly-stiff" phenomenon and provides a *lower* bound solution in energy norm for the exact solution [1]-[2]. In addition, fully compatible FEM usually also has the poor accuracy for stresses especially when the triangular meshes are used. In the past several decades, many assumed strain methods have been made in solving these issues in the framework of FEM [3].

The point interpolation method (PIM) [4]-[8] is one of the meshfree methods [9]-[14] using polynomial basis (or radial basis) shape function with the Kronecker delta function

property. In order to guarantee the stability and the convergence of the PIM, a generalized strain smoothing technique [15] has been proposed based on the weakened weak (W^2) formulation [16]-[17]. Recently, some PIM schemes and techniques have also been proposed and applied to many fields of engineering and sciences [18]-[27].

The node-based smoothed point interpolation method (NS-PIM) [28] is evolved from the point interpolation method (PIM) with the use of gradient smoothing technique [29]. It can guarantee linear accuracy, monotonic convergence, and volumetric locking free. Node-based smoothed finite element method (NS-FEM) [30] is a special case of NS-PIM with linear displacement fields. The detailed discussions and theoretical analysis on the bound properties and convergence for NS-FEM can be found in Ref. [30]. An important property of NS-FEM is that it provides a simple way to obtain an upper solution in energy norm for elasticity problems (with homogenous essential boundary conditions). It has been shown that the node-based smoothing operation can produces a model that is sufficiently "softer" than the real solids, and hence can offer an *upper* bound to the exact solutions.

The important point is that the fully-compatible FEM and the node-based smoothed FEM play complementary roles in the numerical solution bounds: the fully-compatible FEM produces the lower bound solution and NS-FEM produces the upper bound solutions. Hence we have now a general way to bound the solution from the both sides of the exact solution using a usual FEM mesh.

Thus, a question naturally arises: can we develop a method by combining the good features of two methods to improve the accuracy of the numerical solution? In this paper, a strain-constructed hybrid smoothed finite element method (H-SFEM) is proposed using the existing FEM and NS-FEM techniques. A parameter α is equipped into the H-SFEM. By adjusting the parameter, both the upper and lower bound solutions of exact solution can be obtained. Furthermore, a superconvergent solution very close to the exact solution can be obtained for a preferable parameter α_{pre}.

2. The idea of the H-SFEM

The H-SFEM first uses the background cells of 3-node triangles for shape functions construction, which ensures efficiency and reliability. The problem domain Ω is then

divided into a set of smoothing domains Ω_k containing node k as shown in Fig. 1. By connecting node k to the centroids of the surrounding triangles, the Ω_k is further sub-divided into M sub-domains $\Omega_{k,1}$, $\Omega_{k,2}$,…, $\Omega_{k,M}$ and the union of all $\Omega_{k,i}$ forms Ω_k exactly.

Similar to the conventional linear FEM, the displacements in H-SFEM can be approximated as follows.

$$\hat{\mathbf{u}}(\mathbf{x}) = \sum_{i \in n_e} \mathbf{\Phi}_i(\mathbf{x}) \hat{\mathbf{v}}_i \tag{1}$$

where, $\hat{\mathbf{v}}_i$ is the vector of nodal displacements and $\mathbf{\Phi}_i(\mathbf{x})$ is the matrix of the FEM shape functions for node i.

The corresponding compatible strains are

$$\tilde{\boldsymbol{\varepsilon}}(\mathbf{x}) = \mathbf{L}_{\mathrm{d}} \hat{\mathbf{u}}(\mathbf{x}), \tag{2}$$

where $\mathbf{L}_{\mathrm{d}}$ is a matrix of differential operators. For the two-dimensional problem, $\mathbf{L}_{\mathrm{d}}$ is defined as

$$\mathbf{L}_{\mathrm{d}} = \begin{bmatrix} \frac{\partial}{\partial x_1} & 0 & \frac{\partial}{\partial x_2} \\ 0 & \frac{\partial}{\partial x_2} & \frac{\partial}{\partial x_1} \end{bmatrix}^{\mathrm{T}} \tag{3}$$

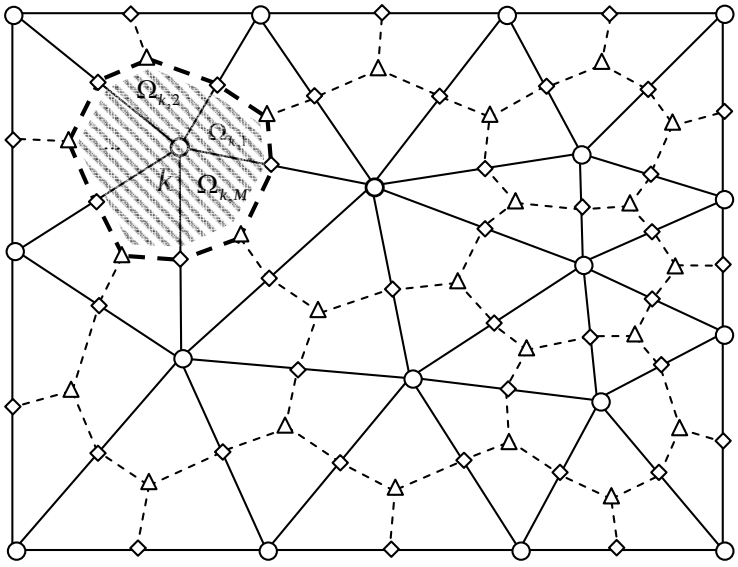

Fig. 1Background elements and the smoothing cells

In the present H-SFEM, the strain $\hat{\boldsymbol{\varepsilon}}$ at any points within any sub-domain $\Omega_{k,i}$ for $k=1,2,...,N$, $i=1,2,...,M$ is assumed to be the linear combination of compatible strain from FEM and smoothed strain from NS-FEM:

$$\hat{\boldsymbol{\varepsilon}}_{k,i}=\alpha\tilde{\boldsymbol{\varepsilon}}_{k,i}+(1-\alpha)\overline{\boldsymbol{\varepsilon}}_{k} \tag{4}$$

where $0\le\alpha\le 1$, $\tilde{\boldsymbol{\varepsilon}}_{k,i}$ is the compatible stain, and

$$\overline{\boldsymbol{\varepsilon}}_{k}=\frac{1}{A_k}\int_{\Omega_k}\tilde{\boldsymbol{\varepsilon}}_{k,i}\mathrm{d}\Omega \tag{5}$$

is the smoothed strain from NS-FEM [30], where A_k is the area of smoothed domain Ω_k.

An extended Galerkin functional is then constructed for variational formulation as:

$$\Pi(\mathbf{v})=\int_{\Omega}\frac{1}{2}\hat{\boldsymbol{\varepsilon}}^{\mathbf{T}}(\mathbf{v})\mathbf{D}\hat{\boldsymbol{\varepsilon}}(\mathbf{v})\Omega-\int_{\Omega}\mathbf{v}^{\mathrm{T}}\mathbf{b}\mathrm{d}\Omega-\int_{\Gamma_t}\mathbf{v}^{\mathrm{T}}\mathbf{T}\mathrm{d}\Gamma \tag{6}$$

where $\mathbf{T}$ is the vector of the prescribed tractions on the natural boundary Γ_{t}, $\mathbf{b}$ is the vector of body forces.

The stationary condition of (6) is

$$\delta\,\Pi(\mathbf{v})=\int_{\Omega}\delta\,\hat{\boldsymbol{\varepsilon}}^{\mathbf{T}}(\mathbf{v})\mathbf{D}\hat{\boldsymbol{\varepsilon}}(\mathbf{v})\Omega-\int_{\Omega}\delta\mathbf{v}^{\mathrm{T}}\mathbf{b}\mathrm{d}\Omega-\int_{\Gamma_t}\delta\mathbf{v}^{\mathrm{T}}\mathbf{T}\mathrm{d}\Gamma=0 \tag{7}$$

Substituting (4) into (7) leads to the discretized system equations as follows

$$\hat{\mathbf{K}}\hat{\mathbf{d}}=\hat{\mathbf{f}} \tag{8}$$

where $\hat{\mathbf{K}}$ is the stiffness matrix, and

$$\hat{\mathbf{f}}=-\int_{\Omega}\boldsymbol{\Phi}^{\mathrm{T}}\mathbf{b}\mathrm{d}\Omega+\int_{\Gamma_t}\boldsymbol{\Phi}^{\mathrm{T}}\mathbf{T}\mathrm{d}\Gamma \tag{9}$$

3. Bound properties of the H-SFEM

The H-SFEM has the following bound properties.

Theorem 1: For any given admissible displacement field $\mathbf{v}$, the strains at any points within sub-domain $\Omega_{k,i}$ are obtained using (4); equation (6) is used to produce discretized system equations. We then have

$$\overline{U}(\mathbf{v})\le\hat{U}(\mathbf{v})\le\tilde{U}(\mathbf{v}) \tag{10}$$

where, $\tilde{U}(\mathbf{v})$ is the strain energy obtained from the FEM solution given by

$$\tilde{U}(\mathbf{v})=\frac{1}{2}\sum_{k=1}^{N}\sum_{i=1}^{M}\left[\int_{\Omega_{k,i}}\tilde{\boldsymbol{\varepsilon}}_{k,i}^{\mathrm{T}}(\mathbf{v})\mathbf{D}\tilde{\boldsymbol{\varepsilon}}_{k,i}(\mathbf{v})\mathrm{d}\Omega\right]; \tag{11}$$

$\bar{U}(\mathbf{v})$ is the strain energy obtained from the NS-PIM solution given by

$$\bar{U}(\mathbf{v})=\frac{1}{2}\sum_{k=1}^{N}\sum_{i=1}^{M}\left[\int_{\Omega_{k,i}}\bar{\boldsymbol{\varepsilon}}_{k}^{\mathrm{T}}(\mathbf{v})\mathbf{D}\bar{\boldsymbol{\varepsilon}}_{k}(\mathbf{v})\mathrm{d}\Omega\right], \tag{12}$$

where N is the number of total nodes in the problem domain.

Proof: For the given displacement, the strain energy from H-SFEM can be written as

$$\begin{aligned}
&\hat{U}(\mathbf{v})\\
&=\sum_{k=1}^{N}\sum_{i=1}^{M}\left[\frac{1}{2}\int_{\Omega_{k,i}}\hat{\boldsymbol{\varepsilon}}_{k,i}^{\mathrm{T}}(\mathbf{v})\mathbf{D}\hat{\boldsymbol{\varepsilon}}_{k,i}(\mathbf{v})\mathrm{d}\Omega\right]\\
&=\sum_{k=1}^{N}\sum_{i=1}^{M}\left[\frac{1}{2}\int_{\Omega_{k,i}}[\alpha\tilde{\boldsymbol{\varepsilon}}_{k,i}+(1-\alpha)\bar{\boldsymbol{\varepsilon}}_{k}]^{\mathrm{T}}\mathbf{D}[\alpha\tilde{\boldsymbol{\varepsilon}}_{k,i}+(1-\alpha)\bar{\boldsymbol{\varepsilon}}_{k}]\mathrm{d}\Omega\right]\\
&=\frac{1}{2}\sum_{k=1}^{N}\sum_{i=1}^{M}\int_{\Omega_{k,i}}[\alpha^{2}\tilde{\boldsymbol{\varepsilon}}_{k,i}^{\mathrm{T}}\mathbf{D}\tilde{\boldsymbol{\varepsilon}}_{k,i}+(1-\alpha^{2})\bar{\boldsymbol{\varepsilon}}_{k}^{\mathrm{T}}\mathbf{D}\bar{\boldsymbol{\varepsilon}}_{k}]\mathrm{d}\Omega\\
&=\alpha^{2}\tilde{U}(\mathbf{v})+(1-\alpha^{2})\bar{U}(\mathbf{v})
\end{aligned} \tag{13}$$

and

$$\hat{U}(\mathbf{v})=\bar{U}+\alpha^{2}\underbrace{(\tilde{U}-\bar{U})}_{\geq 0}=\tilde{U}-(1-\alpha^{2})\underbrace{(\tilde{U}-\bar{U})}_{\geq 0} \tag{14}$$

Note that the fully compatible FEM is "over-stiff", and NS-FEM is "soft". Therefore, we have $\tilde{U}(\mathbf{v})-\bar{U}(\mathbf{v})\geq 0$ for the given displacement **v**, which further indicates from Eq. (14) that $\bar{U}(\mathbf{v})\leq\hat{U}(\mathbf{v})\leq\tilde{U}(\mathbf{v})$ when $0\leq\alpha\leq 1$. This completes the proof. #

Theorem 2: When the same mesh is used, the strain energy obtained from the H-SFEM solution is no-less than that from the FEM solution based on a fully compatible model, and no-larger than the strain potential for the NS-FEM model:

$$\frac{1}{2}\tilde{\mathbf{v}}^{\mathrm{T}}\tilde{\mathbf{K}}\tilde{\mathbf{v}}\leq\frac{1}{2}\hat{\mathbf{v}}^{\mathrm{T}}\hat{\mathbf{K}}\hat{\mathbf{v}}\leq\frac{1}{2}\bar{\mathbf{v}}^{\mathrm{T}}\bar{\mathbf{K}}\,\bar{\mathbf{v}} \tag{15}$$

The proof of Theorem 2 is similar to that in Ref. [28]. For clarity, we give a simple proof as follows.

Proof:

Eqs. (11) and (12) can be written the matrix from as

$$\tilde{U}(\mathbf{v}) = \frac{1}{2}\mathbf{v}^{\mathrm{T}}\tilde{\mathbf{K}}\mathbf{v}, \tag{16}$$

and

$$\bar{U}(\mathbf{v}) = \frac{1}{2}\mathbf{v}^{\mathrm{T}}\bar{\mathbf{K}}\mathbf{v}, \tag{17}$$

where, $\tilde{\mathbf{K}} = \mathbf{L}_{\mathrm{d}}^{\mathrm{T}}\mathbf{D}\mathbf{L}_{\mathrm{d}}$, and $\bar{\mathbf{K}}$ can be found in Ref. [7].

By theorem 1, Eq. (10) can be written in discrete form of arbitrary nodal displacement $\mathbf{v}$ as

$$\frac{1}{2}\mathbf{v}^{\mathrm{T}}\bar{\mathbf{K}}\mathbf{v} \le \frac{1}{2}\mathbf{v}^{\mathrm{T}}\hat{\mathbf{K}}\mathbf{v} \le \frac{1}{2}\mathbf{v}^{\mathrm{T}}\tilde{\mathbf{K}}\mathbf{v} \tag{18}$$

From Eq.(18) , it is easy to see that

$$\frac{1}{2}\mathbf{v}^{\mathrm{T}}(\hat{\mathbf{K}} - \bar{\mathbf{K}})\mathbf{v} \ge 0, \tag{19}$$

$$\frac{1}{2}\mathbf{v}^{\mathrm{T}}(\tilde{\mathbf{K}} - \hat{\mathbf{K}})\mathbf{v} \ge 0. \tag{20}$$

Eqs. (19) and (20) show that matrix $(\hat{\mathbf{K}} - \bar{\mathbf{K}})$ and $(\tilde{\mathbf{K}} - \hat{\mathbf{K}})$ are symmetric and positive definite. In mechanics, it implies that $\hat{\mathbf{K}}$ is "stiffer" than $\bar{\mathbf{K}}$, and "softer" than $\tilde{\mathbf{K}}$.

In addition, the discrete solutions of FEM, NS-FEM and H-SFEM at their stationary points can be written as

$$\tilde{\mathbf{v}} = \tilde{\mathbf{K}}^{-1}\mathbf{f}, \quad \bar{\mathbf{v}} = \bar{\mathbf{K}}^{-1}\mathbf{f}, \quad \hat{\mathbf{v}} = \hat{\mathbf{K}}^{-1}\mathbf{f} \tag{21}$$

where $\mathbf{f}$ is commonly defined by Eq. (9) for all the three models.

At the stationary point we have the total energy as follows

$$\begin{cases} \tilde{\Pi}(\tilde{\mathbf{v}}) = \frac{1}{2}\tilde{\mathbf{v}}^{\mathbf{T}}\tilde{\mathbf{K}}\tilde{\mathbf{v}} - \tilde{\mathbf{v}}^{\mathbf{T}}\mathbf{f} = -\frac{1}{2}\tilde{\mathbf{v}}^{\mathbf{T}}\tilde{\mathbf{K}}\tilde{\mathbf{v}} = -\frac{1}{2}\tilde{\mathbf{v}}^{\mathbf{T}}\mathbf{f} = -\frac{1}{2}\mathbf{f}^{\mathbf{T}}\tilde{\mathbf{K}}^{-1}\mathbf{f} = -\tilde{U}(\tilde{\mathbf{v}}) \\ \bar{\Pi}(\bar{\mathbf{v}}) = \frac{1}{2}\bar{\mathbf{v}}^{\mathbf{T}}\bar{\mathbf{K}}\,\bar{\mathbf{v}} - \bar{\mathbf{v}}^{\mathbf{T}}\mathbf{f} = -\frac{1}{2}\bar{\mathbf{v}}^{\mathbf{T}}\bar{\mathbf{K}}\,\bar{\mathbf{v}} = -\frac{1}{2}\bar{\mathbf{v}}^{\mathbf{T}}\mathbf{f} = -\frac{1}{2}\mathbf{f}^{\mathbf{T}}\bar{\mathbf{K}}^{-1}\mathbf{f} = -\bar{U}(\bar{\mathbf{v}}) \\ \hat{\Pi}(\hat{\mathbf{v}}) = \frac{1}{2}\hat{\mathbf{v}}^{\mathbf{T}}\hat{\mathbf{K}}\hat{\mathbf{v}} - \hat{\mathbf{v}}^{\mathbf{T}}\mathbf{f} = -\frac{1}{2}\hat{\mathbf{v}}^{\mathbf{T}}\hat{\mathbf{K}}\hat{\mathbf{v}} = -\frac{1}{2}\hat{\mathbf{v}}^{\mathbf{T}}\mathbf{f} = -\frac{1}{2}\mathbf{f}^{\mathbf{T}}\hat{\mathbf{K}}^{-1}\mathbf{f} = -\hat{U}(\hat{\mathbf{v}}) \end{cases} \tag{22}$$

The difference between the strain energies of FEM and H-SFEM solution becomes

$$\tilde{U}(\tilde{\mathbf{v}})-\hat{U}(\hat{\mathbf{v}})=\frac{1}{2}\mathbf{f}^{\mathbf{T}}(\tilde{\mathbf{K}}^{-1}-\hat{\mathbf{K}}^{-1})\mathbf{f}\le 0 \tag{23}$$

and the difference between the strain energies of NS-FEM and H-SFEM becomes

$$\bar{U}(\bar{\mathbf{v}})-\hat{U}(\hat{\mathbf{v}})=\frac{1}{2}\mathbf{f}^{\mathbf{T}}(\bar{\mathbf{K}}^{-1}-\hat{\mathbf{K}}^{-1})\mathbf{f}\ge 0 \tag{24}$$

Eqs. (23) and (24) give

$$\tilde{U}(\tilde{\mathbf{v}})\le\hat{U}(\hat{\mathbf{v}})\le\bar{U}(\bar{\mathbf{v}}) \tag{25}$$

This completes the proof. #

Theorem 1 and Theorem 2 indicate that the H-SFEM is bounded by NS-FEM from above and FEM from below. Note that both FEM and NS-FEM are convergent to the exact solution when the dimension of mesh approaches to zero. Therefore, H-SFEM is also convergent to the real solution.

4 Numerical examples and discussions

In this section, a number of numerical examples will be examined using the newly developed H-SFEM. To investigate quantitatively the numerical results, the error indicators in both displacement and energy norms are defined as follows,

$$E_d=\sqrt{\frac{\sum_{i=1}^{n}\left(u_i^{ref}-u_i^{num}\right)^2}{\sum_{i=1}^{n}\left(u_i^{ref}\right)^2}},\quad E_e=\sqrt{\frac{\left|U_{num}-U_{ref}\right|}{U_{ref}}} \tag{26}$$

where the superscript *ref* denotes the reference or analytical solution, *num* denotes a numerical solution obtained using a numerical method.

4.1 Standard path test

For a numerical method working for solid mechanics problems, the sufficient requirement for convergence is to pass the standard path test [1]. Therefore, the first example is the standard path test. A rectangular patch of 10x50 is considered, and the displacements are prescribed on all outside boundaries by the linear function: $u_x=0.6x, u_y=0.6y$. All the errors for any $\alpha\in[0,1]$ in displacement norm defined in (26) are found less than 1.0×10^{-14}. This example demonstrates numerically that the H-SFEM

can pass the standard path test, which at least guarantees linearly conforming.

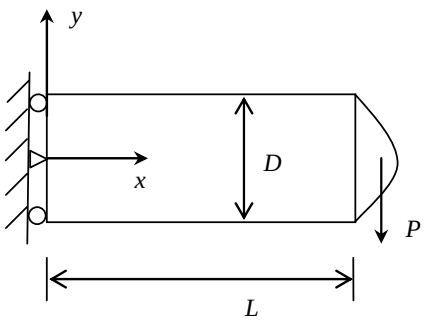

Fig. 2 A 2D cantilever solid with a parabolic traction.

4.2 Cantilever 2D solid

A 2D cantilever solid is now studied as shown in Fig. 2. The solid is subjected to a parabolic traction at the free end, and the analytical solutions can be found in Ref. [31]. To study the convergence property, the strain energy of H-SFEM with linear displacement field for different α is computed and plotted in Fig. 3. It is easy to see that H-SFEM has upper and lower bound solutions when $\alpha = 0.2$, $\alpha = 0.25$ and $\alpha = 0.3$. Furthermore, the strain energy for this model is no-less than those from the compatible FEM solution, and no-larger than the strain potential from the NS-FEM solution. These findings verify the Theorem 2. From this figure, we can also get that $\alpha = 0.25$ leads to a more accurate result than other α.

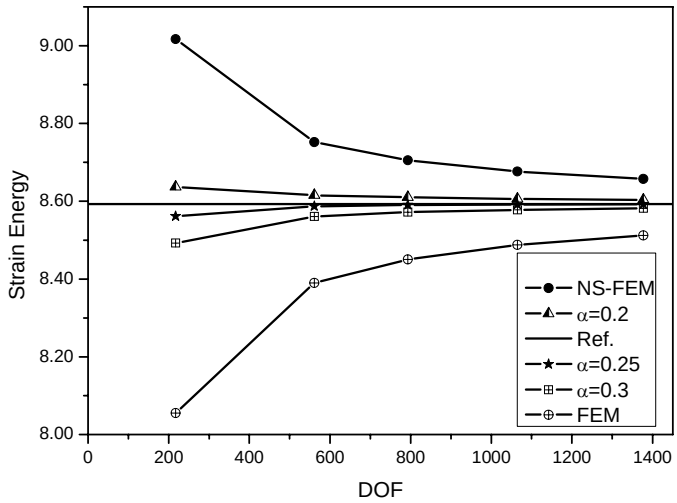

Fig. 3 Solution bounds of the H-SFEM for 2D solid

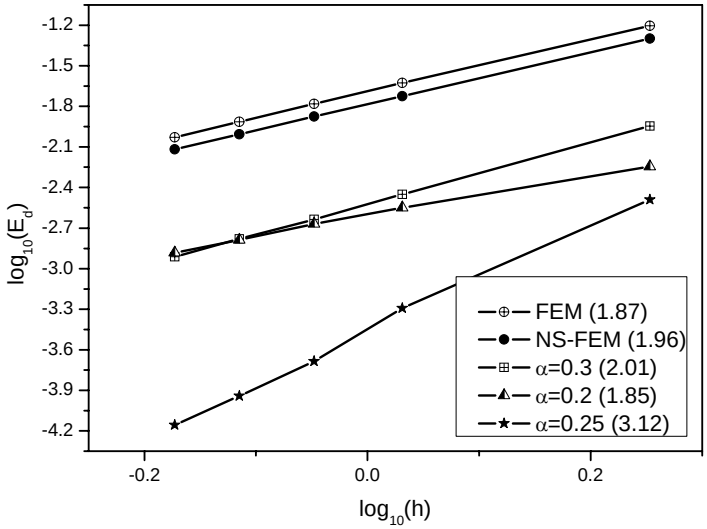

Fig. 4 Displacement error of H-SFEM for 2D solid

Using (26), errors in displacement and energy norms are computed and plotted in Fig. 4 and Fig. 5. When $\alpha = 0.25$, the convergence rates in displacement norm and energy norm are respectively about 3.12 and 1.76, which are much higher than the theoretical values of linear FEM. This shows that we achieved superconvergence in displacement and energy solution.

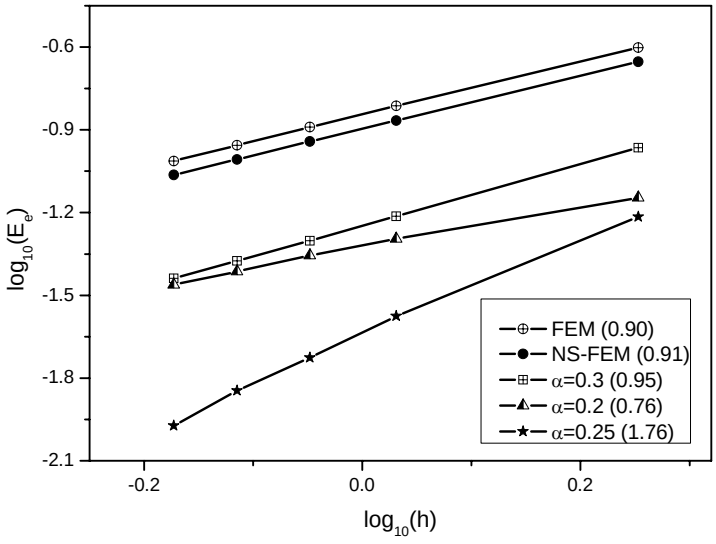

Fig. 5 Energy error of the H-SFEM for 2D solid

4.3 Infinite 2D solid with a circular hole

An infinite 2D solid with a central circular hole and subjected to a unidirectional tensile is studied. Owing to its two-fold symmetry, one quarter is modeled as shown in Fig. 6. The analytical solution of this benchmark problem can be found in Ref. [31]. To study the convergence property, the strain energy of the H-SFEM with linear displacement field for different parameter α are computed and plotted in Fig. 7. It is easy to see that H-SFEM has upper and lower bounds solutions of the exact solution when $\alpha = 0.05, \alpha = 0.18$ and $\alpha = 0.25$, respectively. Furthermore, the strain energy for these model is no-less than that from the compatible FEM solution, and no-larger than the strain potential from the NS-PIM solution.

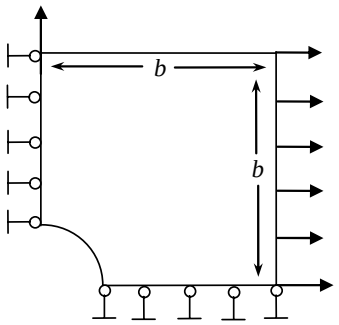

Fig. 6 A quarter model of an infinite 2D solid with a hole.

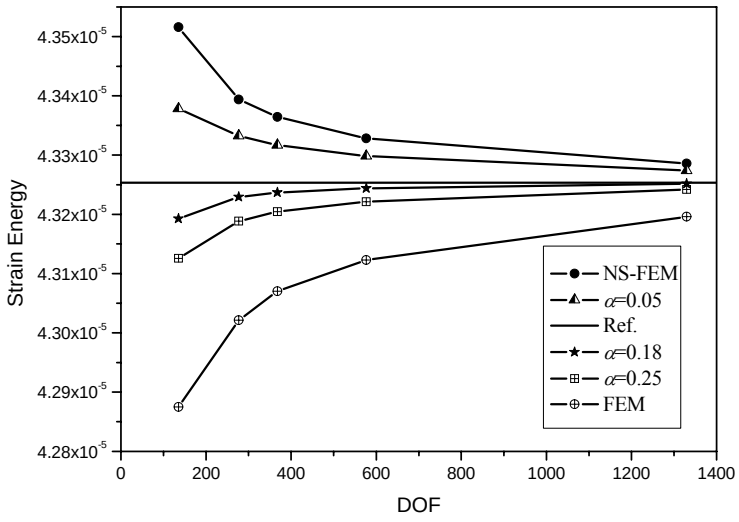

Fig. 7 Solution bounds of the H-SFEM for 2D solid with hole

Using (26), errors in displacement and energy norms are computed and plotted against

the average nodal spacing (h) as shown in Fig. 8 and Fig. 9. It is clear that when $\alpha = 0.18$ the convergence rates in displacement and energy norms are, respectively, about 2.53 and 1.82, which clearly show the superconvergence both the displacement and the energy norms.

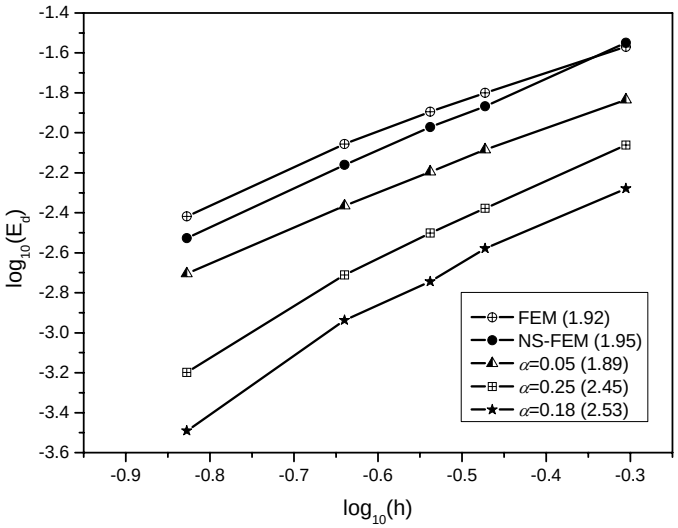

Fig. 8 Displacement error of H-SFEM for 2D solid with hole

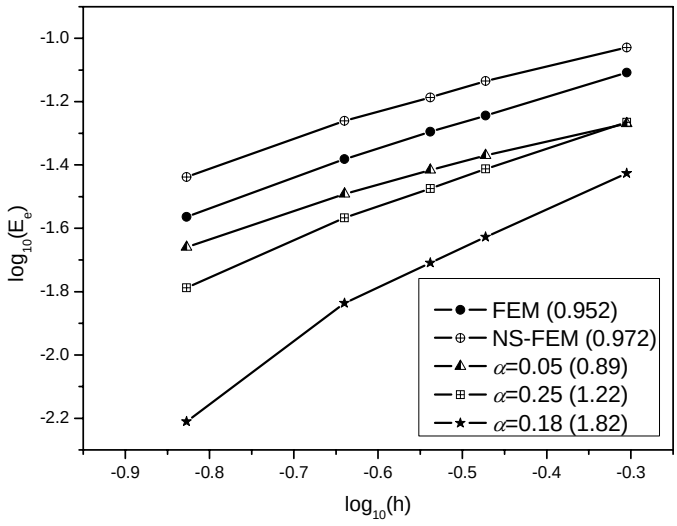

Fig. 9 Energy error of H-SFEM for 2D solid with hole

4.4. The L-shaped Component

An elastic L-shaped component subjected to a pressure load is shown in Fig. 10. Plane stress condition is assumed and the reference solution of strain energy is obtained

using FEM with a very fine mesh. The convergence and energy bound for the H-SFEM are investigated in similar ways as in the previous examples. The computed strain energy and convergent rate in energy norm are plotted in Fig. 11 and Fig. 12, respectively. It is found that the convergent rate in energy norm of H-SFEM is 1.72, and accuracy is also very high which is about 10 times more accurate than that of linear FEM using the same mesh. This further verifies the superconvergence of NS-FEM.

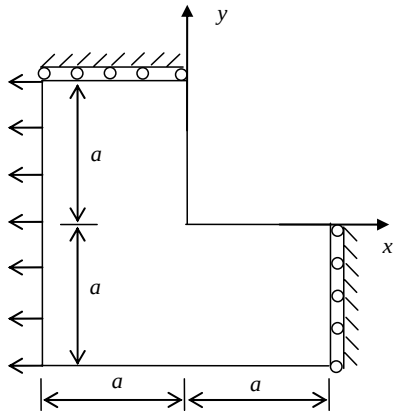

Fig. 10 L-shaped plate subjected to uniform tensile stress.

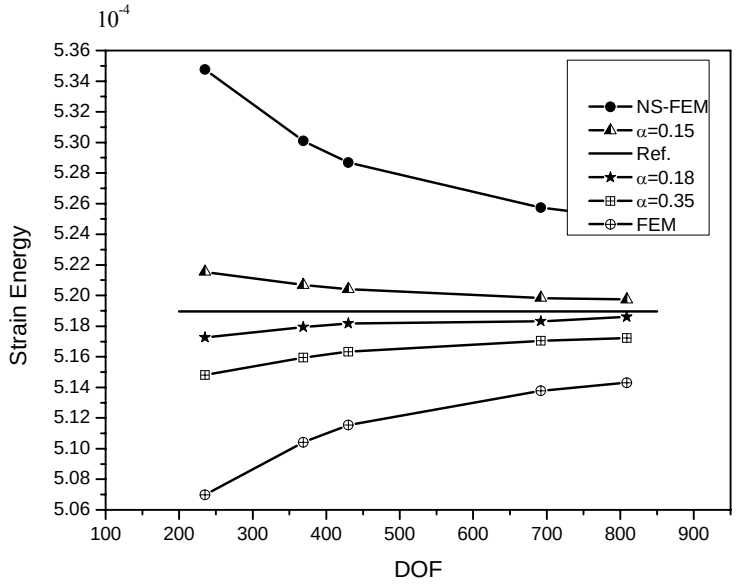

Fig. 11 Solution bound of H-SFEM for L-shaped component

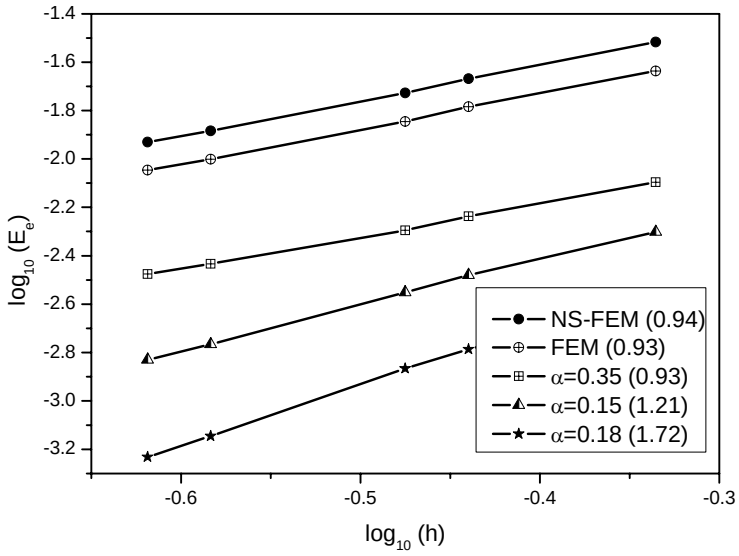

Fig. 12 Energy error of H-SFEM for L-shaped component

4.5. Discussions

From the above discussions, we know that the H-SFEM is equipped with an adjustable parameter α. Both the displacement field $\hat{\mathbf{u}}(\alpha)$ and strain field $\hat{\boldsymbol{\varepsilon}} = (\hat{\mathbf{u}}(\alpha); \alpha)$ are the functions of α. Therefore, an adjustment on α can obviously influence the accuracy and convergence of solutions in *both* displacement and strain energy norms. This is a special superconvergent property that behaves very differently from the fully compatible FEM models. Furthermore, it is known that the solution of the H-SFEM with $\alpha = 1$ is a lower bound of the exact solution in energy norm; while for $\alpha = 0$, it is an upper bound. Thus, there exists a value $\alpha_{pre} \in (0, 1)$ at which the strain energy is very close to the exact solution. Finding such a "prefer" α is ideal; however, it is difficult to find that α for a general problem. Our study has found that such an α_{pre} is in general problem-dependent and also mesh-dependent. To find a "preferable" α that gives a "good" superconvergent solution, the following simple way is recommended [20] .

Our intensive study using numerical examples has discovered an important fact that the α_{pre} is approximately a linear function of the mesh size h for a given model of a problem. We can therefore assume

$$\alpha_{pref}(h) \approx \beta\, h + \gamma \tag{27}$$

where β and γ are unknown and problem-dependent constants. This discovery leads to a simple curve-fitting method to find a preferable $\alpha_{pref}(h)$ that is very close to the α_{exact} for a given problem. The detailed process can be expressed as:

(i). To create a model $M^{(1)}$ with a coarse mesh, and slightly finer model $M^{(2)}$ with elements of the same aspect ratio as model $M^{(1)}$. The nodal spacing of the $M^{(1)}$ and $M^{(2)}$ is denoted as h_1.

(ii). To use $M^{(1)}$ and $M^{(2)}$ to compute and plot two $\hat{U}^{(1)}(\alpha) \sim \alpha$ and $\hat{U}^{(2)}(\alpha) \sim \alpha$ curves;

(iii). To obtain the intersection point $\alpha^{(1)}(h_1)$ of these two curves;

(iv). To repeat (i)-(iii) to obtain another $\alpha^{(2)}(h_2)$ using $M^{(2)}$ and other model $M^{(3)}$ that is slightly finer than $M^{(2)}$ but with the same aspect ratio. The average nodal spacing for these two models is denoted as h_2;

(v). To determine unknown β and γ in Eq. (27) using

$$\beta = \frac{\alpha^{(1)}(h_1) - \alpha^{(2)}(h_2)}{h_1 - h_2} \quad \text{and} \quad \gamma = \alpha^{(1)}(h_1) - \beta\, h_1 \tag{28}$$

When such a "preferable" α is found, the superconvergent solution can be obtained for both the strain energy and the displacement.

We only use the Cantilever 2D solid detailed in Section 4.2 to verify the effectiveness of the above algorithm to find the preferable α. We then compute α_{pref} using the procedures detailed in this Section found $\alpha_{pref}(h) = 0.11h + 0.120$. The convergence rate of H-SFEM in displacement and energy norm, which are illustrated in Figures 13 and 14, respectively about 2.85 and 1.22 when $\alpha = \alpha_{pref}(h)$, which is also much higher even than that of 3-node FEM and 4-node FEM. This example shows clearly the very high accuracy of the solution and excellent superconvergence property of the H-SFEM.

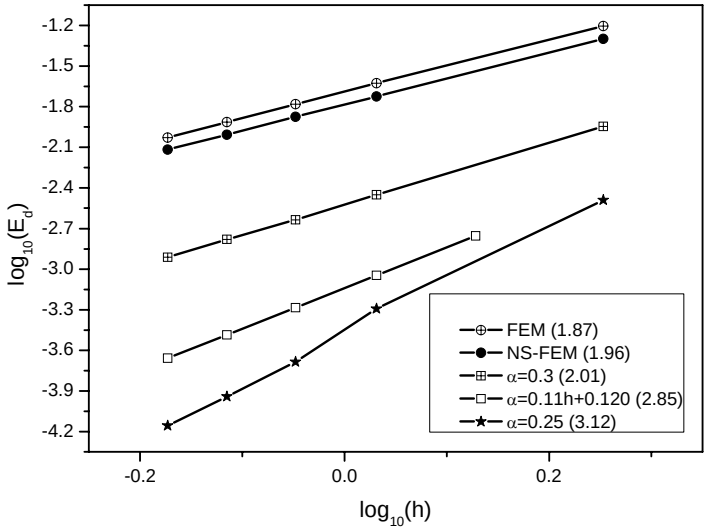

Fig. 13 Displacement error of H-SFEM for 2D solid

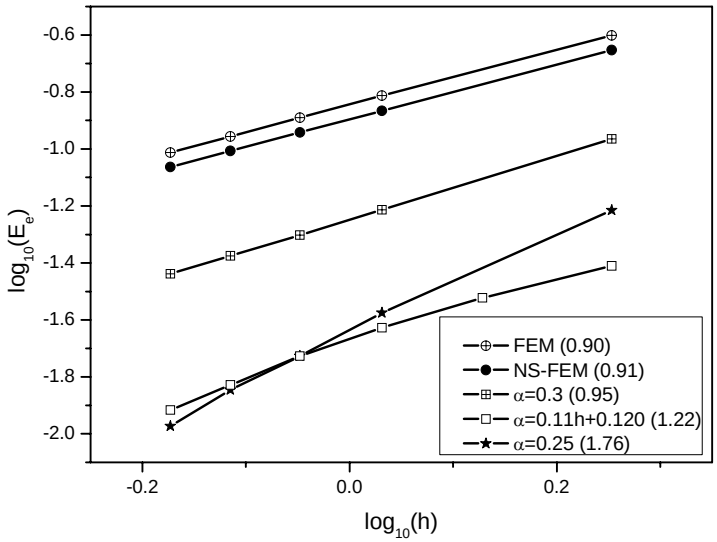

Fig. 14 Energy error of H-SFEM for 2D solid

Comments 1: A disadvantage of the NS-FEM is that it behaves "overly-soft" observed as non-zero energy spurious modes that can result in temporal instability when it is used to solve the dynamic problems, particularly. However, the above numerical examples show that the H-SFEM with preferable parameter α usually produces the upper bound solutions which behave the "overly-stiff" behavior. This phenomenon is confirmed by some other numerical experiments. Therefore, H-SFEM with preferable parameter α

can overcome the "overly-soft' in the NS-FEM and can be used to solve the problems with non-zero energy spurious modes.

Comments 2: In computing the strain field for establishing the stiffness matrix, H-SFEM takes a litter more time compared to the linear FEM and NS-FEM. However, the total CPU time taken is usually dominated by the equation solver especially for large systems; one can expect that the CPU time for a H-SFEM model with a given parameter α will be largely the same as that of NS-FEM using the same mesh. Sections 2 and 3 show that the stiffness matrix in H-SFEM is symmetrical and has the same sparsity and bandwidth compared to the NS-FEM when the same mesh and node number system are used. Hence the solution procedure for the discretized system equations can be exactly the same, and the computational complexity in solving these equations is the same for both NS-FEM and FEM when a direct solver is used. When iterative solver is used, the SC-PIM equations can be solved more efficiently because of the better conditioning in stiffness matrix due to the softening effects.

Comment 3: Equation (4) is used here only for the two-dimensional problems. It can be modified for solving the 3-D problems. In addition, can this method be applied to the dynamic problems and give a superconvergent solution? These two topics will be investigated in our future works.

5 Conclusions

In this paper, a hybrid smoothed finite element method (H-SFEM) is proposed by combining the techniques of the FEM and the NS-FEM using triangular meshes. The following conclusions can be drawn:

1) We have proven theoretically that when the same mesh is used, the strain energy obtained from the H-SFEM solution is no-less than that from the compatible FEM solution and no-larger than the strain potential for the NS-FEM model;

2) The exact solution is bounded by those of H-SFEM with $\alpha = 0$ from above and $\alpha = 1$ from below;

3) There exists an α at which the H-SFEM gives the very high accurate solution in energy norm. A simple algorithm is proposed to determine the preferable α that gives a superconvergent solution.

Intensive numerical studies have verified the convergence, superconvergence and bounds property of the H-SFEM. Hence, H-SFEM is a good candidate to develop a powerful numerical simulation tool for broad applications in computational mechanics.

Acknowledgment

This work was supported in part by the Program for New Century Excellent Talents in University (NCET), by the NSFC under grant number 11072086, by the 985 program, by the 211 project of Jilin University, and by Basic funds for science and research in Jilin University.

References

[1] Zienkiewicz OC, Taylor RL. The Finite Element Method (5th edn). Butterworth Heinemann: Oxford, U.K., 2000.

[2] Liu GR, Quek SS, The finite Element Method: a Practical Course. Butterworth Heinemann: Oxford, 2003.

[3] Pian Thh, Wu CC, Hybrid and Incompatible Finite Element Methods, CRC Press: Boca Raton, FL, 2006.

[4] Liu GR, Gu YT, A point interpolation method for two-dimensional solids. International Journal for Numerical Methods in Engineering, 2001; 50(4): 937-951.

[5] Gu YT, Meshfree methods and their comparisons. International Journal of Computational Methods (IJCM) (Special issue, eds.: Gu and Worsak), 2005; 2(4): 477-515.

[6] Liu GR and Gu YT, Assessment and applications of point interpolation methods for computational mechanics, International Journal for Numerical Methods in Engineering, 2004; 59: 1373–1397.

[7] Liu GR, Meshfree methods: Moving beyond the Finite Element Method. CRC Press: Boca Raton, U.S.A, 2002.

[8] Liu GR, Zhang GY, Dai KY, Wang YY, Zhong ZH, Li GY, Han X, A linearly conforming point interpolation method (NS-PIM) for 2D solid mechanics problems. International Journal of Computational Methods, 2005; 2: 645–665.

[9] Belytschko Y, Lu YY and Gu L. Element-free Galerkin methods. International Journal for Numerical Methods in Engineering, 1994; **37**:229–256.

[10] Liu WK, Jun S and Zhang YF. Reproducing kernel particle methods. International Journal for Numerical Methods in Engineering, 1995; **20**:1081–1106.

[11] Atluri SN and Zhu T. A new meshless local Petrov–Galerkin (MLPG) approach in computational mechanics. Computational Mechanics, 1998; **22**:117–127.

[12] Nayroles B, Touzot G and Villon P. Generalizing the finite element method: diffuse approximation and diffuse elements. Computational Mechanics, 1992; **10**:307–318.

[13] Lucy LB. A numerical approach to testing the fission hypothesis. The Astronomical Journal 1977; **8**(12): 1013–1024.

[14] Gu L, Moving Kriging interpolation and element-free Galerkin method, International Journal for Numerical Methods in Engineering, 2003; 56: 1-11.

[15] Liu GR, A generalized gradient smoothing technique and the smoothed bilinear form for Galerkin formulation of a wide class of computational methods, International Journal of Computational Methods, 2008; **5**(2):199–236.

[16] Liu GR. A G space theory and a weakened weak (W2) form for a unified formulation of compatible and incompatible methods: Part I: Theory. Applications to solid mechanics problems, International Journal for Numerical Methods in Engineering, 2010; **81**: 1093-1126.

[17] Liu GR. A G space theory and a weakened weak (W2) form for a unified formulation of compatible and incompatible methods: Part II applications to solid mechanics problems. International Journal for Numerical Methods in Engineering, 2010; **81**: 1127-1156.

[18] Liu G R, Nguyen-Thoi T, Lam K Y. An edge-based smoothed finite element method (ES-FEM) for static, free and forced vibration analyses in solids. Journal of Sound and Vibration, 2009; **320**: 1100-1130.

[19] Liu G R, Zhang G Y. A novel scheme of strain-constructed point interpolation method for static and dynamic mechanics problems, International Journal of Applied Mechanics, 2009; **1**(1): 233-258.

[20] Liu G R, Xu X, Zhang G Y, Nguyen-Thoi T, A superconvergent point interpolation method (SC-PIM) with piecewise linear strain field using triangular mesh. International Journal for Numerical Methods in Engineering, 2009; **77**: 1439-1467.

[21] Liu G R, Xu X, Zhang G Y, Gu Y T, An extended Galerkin weak form and a point interpolation method with continuous strain field and superconvergence using triangular mesh. Computational Mechanics, 2009; **43**: 651-673.

[22] Xu X, Liu GR, Gu YT and Zhang GY, A conforming point interpolation method (CPIM) by shape function reconstruction for elasticity problems, International Journal of Computational Methods, 2010; **7**(3): 369-395.

[23] Xu X, Liu GR, Gu YT, Zhang GY, A conforming point interpolation method (CPIM) by shape function reconstruction for elasticity problems, International Journal of Computational Methods, 2010, 7(3): 369-395.

[24] Xu X, Liu GR, Gu YT, Zhang GY, A point interpolation method with least square strain field (PIM-LSS) for solution bounds and ultra-accurate solutions using triangular mesh, Computer Methods in Applied Mechanics and Engineering, 2009, 198,1486-1499.

[25] Liu G Ru, Nguyen-Xuan H, Nguyen-Thoi T, Xu X, A novel Galerkin-like weakform and a super-convergent alpha finite element method (S_FEM) for mechanics problems

using triangular meshes, Journal of Computational Physics, 2009; 228 (11-20) : 4055-4087.

[26] Nguyen-Thanh N, Rabczuk T, Nguyen-Xuan H, Bordas S, An alternative alpha finite element method (A_FEM) for free and forced structural vibration using triangular meshes, Journal of Computational and Applied Mathematics, 2010; 233(9): 2112-2135.

[27] Nguyen-Thanh N, Rabczuk T, Nguyen-Xuan H, Bordas S. An alternative alpha finite element method with stabilized discrete shear gap technique for analysis of Mindlin-Reissner plates, Finite Elements in Analysis and Design, 2011; 47(5):519-535.

[28] Liu GR, Zhang GY, Upper bound solution to elasticity problems: A unique property of the linearly conforming point interpolation method (NS-PIM), International Journal for Numerical Methods in Engineering, Vol. 74, pp.1128-1161, 2008.

[29] Chen JS, Wu CT, Yoon S and You Y, A stabilized conforming nodal integration for Galerkin mesh-free methods, International Journal for Numerical Methods in Engineering, 2001; **50**: 435–466.

[30] Liu GR, Nguyen-Thoi T, Nguyen-Xuan H, Lam, KY, A node-based smoothed finite element method (NS-FEM) for upper bound solutions to solid mechanics problems, Computers and Structures, 2009; **87**: 14-26.

[31] Timoshenko SP, Goodier JN. Theory of Elasticity (3rd edn). McGraw: New York, 1970.